Transportmetrica B: Transport Dynamics

ISSN: 2168-0566 (Print) 2168-0582 (Online) Journal homepage: http://www.tandfonline.com/loi/ttrb20

Path-based MAXBAND with green-split variables and traffic dispersion

H.-J. Cho, T.-J. Huang & C.-C. L. Huang

To cite this article: H.-J. Cho, T.-J. Huang & C.-C. L. Huang (2018): Path-based MAXBAND with green-split variables and traffic dispersion, Transportmetrica B: Transport Dynamics, DOI: 10.1080/21680566.2018.1493624

To link to this article: https://doi.org/10.1080/21680566.2018.1493624

Published online: 10 Jul 2018.

TRANSPORTMETRICA B: TRANSPORT DYNAMICS
https://doi.org/10.1080/21680566.2018.1493624

Taylor & Francis
Taylor & Francis Group

Path-based MAXBAND with green-split variables and traffic dispersion

H.-J. Cho[a], T.-J. Huang[a] and C.-C. L. Huang[b]

[a]Department of Transportation and Logistics Management, National Chiao Tung University, Hsinchu, Taiwan;
[b]College of Management, National Kaohsiung University of Science and Technology, Kaohsiung, Taiwan

ABSTRACT

In this paper, we propose two path-based MAXBAND models for solving signal synchronization problems for coordinated traffic signalization systems. In the first proposed model (RM1), we relax the assumptions that the lengths of the common cycle, as well as the green splits, are fixed in the base path-based MAXBAND model. These two factors are considered as decision variables in RM1, which leads us to a generalized offset optimization problem. In the second model (RM2), we further relax the free-flow speed assumption used for estimating the link travel times in the coordinated system. Since the free-flow speed can only be reached in rare occasions, we, instead, adopt the Robertson's dispersion module for this purpose. Proposed methodologies are applied to solving a real-world application in that a pure-traffic arterial system in Chubei city, Taiwan, is analyzed for performance evaluations. Numerical results suggest significant improvements from the proposed models, compared to plans suggested by the governmental authority and the literature. From path-wise perspective, model RM1 and RM2 are nip-and-tuck alternatives. From an aggregate perspective, model RM2 has the best performance among all alternatives, with overall improvements around 40%.

ARTICLE HISTORY
Received 8 August 2017
Accepted 23 June 2018

KEYWORDS
Signal synchronization; traffic progression; urban traffic

1. Introduction

An effective signal control strategy is crucial in improving the LoS for coordinated signalized intersections. By adjusting the offsets of the coordinated intersections in an arterial system, the control delays and the stopping times of vehicles can be well controlled, thereby providing better LoS. This is particularly true for arterial systems serving as the connectors of highway ramp systems and surface traffic networks in many cities around the world. Congestions are frequently taking place simply because the signal control strategies for such systems are barely satisfactorily set in response to the varying traffic nowadays. Manpower is oftentimes needed and is stationed at congested intersections to manage the traffic flow during the rush hours. Such a costly decision can be evaded, provided there is a good control strategy involved. Therefore, developments of more sophisticated and practically useful techniques and/or models for solving the signal control problems and for providing better control strategies are urgently needed.

The concept of MAXBAND model, proposed by Morgan and Little (1964), is one effective approach for this purpose. A typical MAXBAND model is to maximize the total progression band of a two-way

CONTACT C.-C. L. Huang liamplayt@nkfust.edu.tw, liamplayt@gmail.com

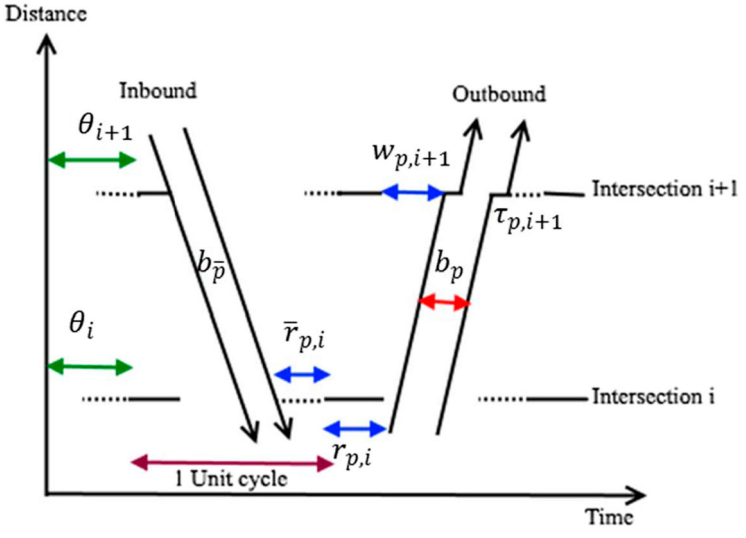

Figure 1. Geometric presentation for the MAXBAND model.

coordinated signalized system by adjusting the offsets at all intersections over a given time interval. Mathematical formulations of the MAXBAND model, encompassing time constraints describing temporal relationship between the upstream and downstream intersections, was later completed by Little (1966) and formulated as a mixed-integer linear programming problem (MILP), see Figure 1 for a geometric reference. Several extensions were later proposed by traffic professionals and interested researchers. Chang et al. (1988) proposed the MAXBAND-86 that extends Little's model to solve multi-arterial closed network problems. Yet, neither model has taken the lead-lag left-turning phases and the queuing clearance times into account. Gartner et al. (1991) solved the problem by developing a multiband model that incorporates the left-turning phase sequence optimization and initial queue clearance times. The major contribution of multiband model resides in the consideration of the flow volume in the model.

Based on the multiband model, Stamatiadis and Gartner (1996) proposed the Multiband-96 model, extending the multiband model to arterial networks. Gartner and Stamatiadis (2002) studied the MAXBAND problem with uniform and variable bandwidths. A network generalization was also discussed. Shoufeng, Ximin, and Shiqiang (2008) extended the multiband model by incorporating the travel time constraints with traffic dispersion module (Robertson 1969). This relaxes the assumption that the link travel time is calculated based on the free-flow speed. Zhang et al. (2015) improved Gartner's model by relaxing the limitation of symmetrical progression. In other words, the progression band is no longer required to be symmetric in the time-space diagram. One restriction of all these models above is that they do not consider the arterial system containing turning flow from minor legs crossing the arterial. In this case, even though the efficiency of the arterial system is improved, the efficiency of the entire network may not be the case necessarily. Most recently, based on the critical-path concept from Tseng (2012), Yang, Cheng, and Chang (2015) proposed multi-path progression models featuring the optimization of the phase sequences and the determination of critical paths in the associated network. Their models can handle the intersections with high turning volumes on the minor legs by adding a new path through the arterial. Also, by adding more constraints, their model is capable of removing unnecessary paths with zero bandwidth. In the same year, Dai, Wang, and Wang (2015) proposed a bandwidth model for the signal synchronization problem, by taking into consideration the bus priority. Their approach can generate green bands for both bus systems and general vehicles with the same timing plan. Simulation results suggest significant improvements in the system performance.

1.1. Our Contributions

Major restrictions in the progression model proposed by Yang, Cheng, and Chang (2015) reside in that the length of the common cycle, as well as the phases comprising it for the coordinated intersections are fixed. Such a restriction can lead to unsatisfactory local solutions because the solution space is highly restricted. Therefore, this paper presents extensions of their models by relaxing such restrictions so that the lengths of phases in a cycle, as well as the cycle itself, become variable. Such flexibilities can move us out of the restricted local solution region and lead to potentially better solutions, compared to the fixed case. Consequently, the resultant model becomes a mixed-integer quadratically constrained programming (MIQCP) problem which is NP-hard (Pardalos 1991) in essence. Thanks to the strong capability of commercial optimization software, the search for an approximate feasible solution can therefore be done.

Besides, the computation of link travel times in most of the literature is based upon the assumption that the link travel speeds are fixed, oftentimes assumed at the free-flow speed. Such an assumption can be very unrealistic, especially when the free-flow speed is seldom met in most circumstances. To this problem, we adopt the traffic dispersion module (Robertson 1969) to account for link travel times from one intersection to the downstream one, thereby providing more realistic results.

1.2. Organization

This is how the rest of the paper is organized. In Section 2, we review the path-based MAXBAND model proposed by Yang, Cheng, and Chang (2015). We start by defining variables and parameters relevant to the formulation and give explanations on the model formulation thereafter. In Section 3, we point out the major restrictions of the base model in Section 2, and propose the first extended model RM1 by relaxing the restrictions on timing-plan parameters. Important theoretical assertions are made. In Section 4, we further replace the free-flow speed assumption, used for estimating link travel times in the MAXBAND models, with the traffic dispersion module in the TRANSYT family to account for a better time estimation. The relationship between the base and the extended models are given.

In Section 5, we elaborate on how the proposed methodologies are applied to a real-world signal synchronization problem in Taiwan. Real traffic data, such as traffic volume, timing plan and so on, are used as the input to the proposed models. Numerical simulations are performed by using the traffic simulation software TSIS and the results are given and analyzed in Section 6. Lastly, the conclusions are given in Section 7.

2. Review of multi-path progression model

Model M2 is an optimization problem concurrently optimizing the phase sequences and offsets and is formulated as a mixed-integer linear programming (MILP) problem. This model maximizes the total progression bands and is subject to certain temporal constraints with respect to a set of chosen paths.

Let now $P = \{p : p \in \mathbb{N}\}$ and $\bar{P} = \{\bar{p} : \bar{p} \in \mathbb{N}\}$ be the sets of outbound and inbound paths selected for optimization, respectively. Unless otherwise specified, all defined variables and parameters, coming with a subscript $p \in P$, will have their own analogs with respect to $\bar{P}$. Define b_p as the total bandwidth for the outbound path $p \in P$, associated with the weight parameter φ_p. Let $w_{p,i}$ ($\bar{w}_{\bar{p},i}$) be the time from the right (left) side of the outbound (inbound) path at intersection i; $r_{p,i}$ ($\bar{r}_{p,i}$) be the left-(right-)end red time of the band in a cycle; $\tau_{p,i}$ be the queue clearance time of path p at intersection i; and $m_{p,i}$ be an integer variable. Let $\phi_{l,i}$ be the ratio of phase l to a cycle at intersection i. Let θ_i be the offset at intersection i, and t_i be the travel time from intersection i to intersection i+1. We define a binary variable $\beta_{p,l,i}$ taking on value 1 if path p is on the green light in the phase l at intersection i; and 0, otherwise. Binary variable $x_{l,m,i}$ takes on value 1 if the phase l precedes phase m at intersection i; and 0, otherwise. Figure 1 visualizes the temporal relationship among the time variables in a MAXBAND model.

Decision variables include the bandwidth variables (b_p, $b_{\bar{p}}$), the interference variables ($w_{p,i}$, $\bar{w}_{\bar{p},i}$), the green split ($\phi_{l,i}$), the left-(right-)end red times ($r_{p,i}$, $\bar{r}_{p,i}$, $r_{\bar{p},i}$, $\bar{r}_{\bar{p},i}$,), the offset (θ_i), the loop variable ($m_{p,i}$, $m_{\bar{p},i}$), and the binary variable ($x_{l,m,i}$). Model parameters include the weights of bandwidth (φ_p, $\varphi_{\bar{p}}$), the binary variable ($\beta_{p,l,i}$, $\beta_{\bar{p},l,i}$), travel time (t_i, $\bar{t}_i$), and the queue clearance time ($\tau_{p,i}$, $\tau_{\bar{p},i}$). M is a penalty parameter.

The objective function (1) is to maximize the weighted sum of bandwidths of outbound (P) and inbound paths ($\bar{P}$). Mathematically, we write

$$\max \sum_{p} \varphi_p b_p + \sum_{\bar{p}} \varphi_{\bar{p}} b_{\bar{p}} \tag{1}$$

The weighting parameters φ_p and $\varphi_{\bar{p}}$ can be adjusted according to the relative importance of the associated paths in the network. In this paper, all paths are considered equal, *viz.*, $\varphi_p = \varphi_{\bar{p}} = 1$, for all $p \in P$ and $\bar{p} \in \bar{P}$.

Since the goal of model M2 is to solve for a timing plan, temporal constraints are imposed to ensure feasibility in the time-space diagram (Morgan and Little 1964). Moreover, because the model is a path-based model, all constraints are set with respect to path. Constraints (2) and (3) are interference constraints that guarantee the sum of the interference time and the green band will not exceed the total green time in a cycle, *viz.*,

$$w_{p,i} + b_p \le \sum_{l} \beta_{p,l,i} \phi_{l,i}, \quad \text{for} \quad p \in P \quad \text{and} \quad \forall\, i \tag{2}$$

$$w_{\bar{p},i} + b_{\bar{p}} \le \sum_{l} \beta_{\bar{p},l,i} \phi_{l,i} \quad \text{for} \quad \bar{p} \in \bar{P} \quad \text{and} \quad \forall\, i \tag{3}$$

In other words, the progression band of path p ($\bar{p}$) will only use the available green time at intersection i.

Since the model is designed to synchronize the signals in a coordinated traffic system, we must ensure that the synchronization between the upstream and the downstream intersections is well set. This is done by adding the loop constraints (4) and (5), representing the synchronizing relationship between intersection i and i+1 while they are synchronized. Thus, we have

$$\theta_i + r_{p,i} + w_{p,i} + t_i + m_{p,i} = \theta_{i+1} + r_{p,i+1} + w_{p,i+1} + \tau_{p,i+1} + m_{p,i+1} \tag{4}$$

$$-\theta_i + \bar{r}_{\bar{p},i} + w_{\bar{p},i} - \tau_{\bar{p},i} + \bar{t}_i + m_{\bar{p},i} = -\theta_{i+1} + \bar{r}_{\bar{p},i+1} + w_{\bar{p},i+1} + m_{\bar{p},i+1} \tag{5}$$

Note that, for the outbound paths, one need only consider the left-side red time, as in Equation (4); while for the inbound paths, one need only consider the right-side red time, as in Equation (5).

The red times in a cycle are also needed to be addressed. Constraints (6)–(11) are the boundary conditions for the left/right-side red times of progression band.

$$r_{p,i} \le \sum_{l} \beta_{p,m,i} x_{l,m,i} \phi_{l,i} + M(1 - \beta_{p,m,i}), \quad \forall\, m \tag{6}$$

$$\bar{r}_{p,i} \le \sum_{l} \beta_{p,m,i} x_{m,l,i} \phi_{l,i} + M(1 - \beta_{p,m,i}), \quad \forall\, m \tag{7}$$

$$r_{p,i} + \bar{r}_{p,i} + \sum_{l} \beta_{p,l,i} \phi_{l,i} = 1, \quad \forall\, p \in P \tag{8}$$

$$r_{\bar{p},i} \le \sum_{l} \beta_{\bar{p},m,i} x_{l,m,i} \phi_{l,i} + M(1 - \beta_{\bar{p},m,i}), \quad \forall\, m \tag{9}$$

$$\bar{r}_{\bar{p},i} \leq \sum_{l} \beta_{\bar{p},m,i} x_{m,l,i} \phi_{l,i} + M(1 - \beta_{\bar{p},m,i}), \quad \forall\, m \tag{10}$$

$$r_{\bar{p},i} + \bar{r}_{\bar{p},i} + \sum_{l} \beta_{\bar{p},l,i} \phi_{l,i} = 1, \quad \forall\, \bar{p} \in \bar{P} \tag{11}$$

Specifically, constraints (8) and (11) say that the left- and right-end red times plus green time constitute the entire cycle for outbound and inbound paths, respectively. Further, constraints (6)–(7) and (9)–(10) are effective only when the binary variable $\beta_{\bullet,m,i}$ is active. Note that constraints (6)–(11) are set for all intersections.

Lastly, the order of phases is allowed to be adjusted, which can be done by exploiting the concept of relative positions. Constraints (12)–(17) describes the positioning relationship of any two phases in a cycle. These constraints are set to ensure the feasibilities of the phases sequences.

$$x_{l,l,i} = 0, \quad \forall\, l \tag{12}$$

$$x_{l,m,i} + x_{m,l,i} = 0, \quad \forall\, l \neq m, \quad \text{and} \quad \forall\, i \tag{13}$$

$$x_{l,n,i} \geq x_{l,m,i} + x_{m,n,i} - 1, \quad \forall\, l \neq m \neq n, \quad \text{and} \quad \forall\, i \tag{14}$$

$$x_{l,n,i} + x_{n,m,i} = 1, \quad \forall\, l \neq m \neq n, \quad \text{and} \quad \forall\, i \tag{15}$$

$$x_{l,m,i} = 1, \quad \forall\, l \neq m, \quad \text{and} \quad \forall\, i \tag{16}$$

$$x_{l,m,i} - x_{l',m',i} = 0, \quad \forall\, i \tag{17}$$

According to Yang, Cheng, and Chang (2015), constraints (15)–(17) are optional in the model.

3. Green split as variables

One major restriction in model M2 is that the timing operations are considered parameters. Mathematically speaking, the durations of phases to a cycle, and thus the cycle length, are fixed, *viz.*, $\phi_{l,i}$'s are constant. Such a restricted leads us to the predicament that the solution space is highly confined in a local region. Hence, even though one may find a good quality solution within this region, the opportunity to get a better solution is basically lost. If we can relax such a restriction by letting the ratios $\phi_{l,i}$'s become variables, then the solution space is enormously enlarged and we have more chances to search for better solutions, because doing so can move us out of the local region, thereby improving the quality of the results.

Yet, such a relaxation costs a price that it introduces more complexities to the problem. One complexity results from the settings of ratio variables in the sense that the original MILP problem has become a mixed-integer quadratically constrained programming (MIQCP) problem. The difficulty of solving MIQCP problems can be expected, and devising an algorithm or heuristic for solving the problem is beyond our purpose. Thus, we shall resort to commercial optimization solvers for obtaining an approximate feasible solution.

Another complexity comes from additional constraints needed for feasibility consideration. Since we are adding more variables to the problem, we must ensure that the addition of these variables does not lead us to infeasibility. Since the ratio $\phi_{l,i}$ has become variable, we need to ensure that the ratios constitute the entire cycle. In other words, the sum of the ratios must equal 1, which we write

$$\sum_{l} \phi_{l,i} = 1, \quad \forall\, i \tag{18}$$

As aforementioned, the revised model is an MIQCP. According to Jeroslow (1973), an MIQCP is solvable if and only if a proper lower bound is set. For this purpose, we resort to the capacity formula discussed

in Roess, Prassas, and McShane (2011). The capacity equation describes the mathematical relationship between the capacity and the ratio of effective green to a cycle, *viz.,*

$$c_q = \frac{s_q g_q}{C} \Rightarrow \frac{c_q}{s_q} = \frac{g_q}{C} \tag{19}$$

where c_q is the capacity for lane or lane group q; s_q is the saturation flow rate for lane or lane group q; g_q is the effective green time for lane or lane group q; and the C is the cycle length. Since the critical volume of lane q, V_q^c, is always less than or equal to the capacity thereof, we have $c_q \geq V_q^c$. Moreover, the ratio $\frac{g_q}{C}$ on the right-hand side of the equality in (19) is the ratio of the green time to the cycle, *viz.,* ϕ_q. Together, we get

$$\phi_q = \frac{g_q}{C} = \frac{c_q}{s_q} \geq \frac{V_q^c}{s_q} \tag{20}$$

Consequently, from the above, we obtain the following lower bounds for the revised MIQCP

$$\phi_{l,i} \geq \frac{V_{l,i}^c}{s}, \quad \text{for} \quad \sum_l \frac{V_{l,i}^c}{s} \leq 0.925 \tag{21}$$

and

$$\phi_{l,i} \geq \frac{\frac{V_{l,i}^c}{s}}{\sum_l \frac{V_{l,i}^c}{s} + 0.075}, \quad \text{for} \quad \sum_l \frac{V_{l,i}^c}{s} > 0.925 \tag{22}$$

where the threshold 0.925 is a given parameter set to evade over-saturation, and the remaining proportion of the cycle is left for further adjustments, if needed. The following result holds.

Proposition 3.1: *Constraints* (21) *and* (22) *are valid.*

Proof: For constraint (21), we see that

$$1 = \sum_l \phi_{l,i} \geq \sum_l \frac{V_{l,i}^c}{s} \tag{23}$$

which is always true for the condition $\sum_l V_{l,i}^c/s \leq 0.925$. As to constraint (22), it follows that

$$\frac{\frac{V_{l,i}^c}{s}}{\sum_l \frac{V_{l,i}^c}{s} + 0.075} < \frac{V_{l,i}^c}{s} \leq \phi_{l,i} \tag{24}$$

which is exactly the constraint itself. ■

We remark on the condition in constraint (21). The value 0.925 is set based on our experiences when observing the random simulations in TSIS. The value may vary highly depending on particular applications. For different arterial systems, the values are supposed to be different.

The length of the common cycle is also a variable in our model. To retain feasibility in this aspect, we impose lower and upper bounds on the reciprocal of the common cycle length Z and write

$$\frac{1}{e} \leq Z \leq \frac{1}{f} \tag{25}$$

where e and f are, respectively, the upper and lower bounds of the cycle length. With this constraint, the link travel time from intersection i to intersection $i+1$ can then be reformulated as

$$t_i = \frac{d_i}{v_i} Z \tag{26}$$

and

$$\bar{t}_i = \frac{\bar{d}_i}{\bar{v}_i} Z \tag{27}$$

where d_i ($\bar{d}_i$) is the distance between intersection i and intersection $i+1$; and v_i ($\bar{v}_i$) is the free-flow speed.

Summing up, the first proposed model, named RM1, combines the base model with the additional constraints (18), (21)–(22) and (25)–(27). In addition, as suggested by Yang, Cheng, and Chang (2015), constraints (15)–(17) will not be considered.

Before ending the discussion, we note that if we let the green split $\phi_{l,i}$ as well as the common cycle length in RM1 be constants, then RM1 reduces to the original base model. Specifically, we claim the following result to be true.

Theorem 3.2: *Model M2 is a special case of RM1*

Proof: This is obvious by setting the cycle length variable Z and the green split ϕ to constants in RM1, which leads to M2. ■

A more formal version of the above theorem is given below.

Theorem 3.3: *Suppose g^* is an optimal solution to Model M2, then g^* is a feasible solution to RM1 and the objective function value, say $f(g^*)$, is a lower bound to RM1.*

Proof: Since g^* is an optimal solution to M2, it suffices to check if constraints (18), (21)–(22) and (25)–(27) in RM2 are satisfied. Obviously, (18) and (25)–(27) are fine. Constraints (21)–(22) are met due to Proposition 3.1. This implies that g^* is indeed a feasible solution to RM1 and thus $f(g^*)$ is a lower bound. ■

4. Incorporating traffic dispersion

In the first proposed model, the link travel time from intersection i to intersection $i+1$ is defined as the ratio of the distance in between to the free-flow speed of that link, as in constraints (26) and (27). In the context of MAXBAND models, there are in general two approaches to deal with the speed parameters, one of which is to make it a constant, and the other of which is to set boundary conditions for it (Little 1966). Yet, two approaches have their disadvantages. For the first approach, on the one hand, the free -flow speed can seldom be reached in most circumstances, especially when the traffic is far from being sparse. On the other hand, assuming that the link travel time for all traffic remains constant is far from being realistic. For the second approach, it requires the introduction of new variables to the model, resulting in more complexities.

Based on these observations, we resort to the traffic dispersion module introduced in the TRANSYT family by Robertson (1969) for computing the link travel times. The dispersion module ensembles

computing the expectation of geometric variables to estimate the link travel time. The travel time can be adjusted in accordance with the upper and lower travel speeds on that link. For the upper travel speed, the free-flow speed or the speed limit of that link is used. As for the lower travel speed, since there usually is no lower speed limit for urban traffic systems, the bound is set based on the simulation results from TSIS program. In other words, the lower travel speed may vary depending on particular applications.

Consequently, the outbound (t_s) and inbound travel times ($\bar{t}_s$) can be computed through the following equations

$$t_i = \sum_{T_i=t_f}^{t_s} T_i F(1-F)^{T_i - t_f} Z \tag{28}$$

and

$$\bar{t}_i = \sum_{T_i=\bar{t}_f}^{\bar{t}_s} T_i F(1-F)^{T_i - \bar{t}_f} Z \tag{29}$$

where t_f ($\bar{t}_f$) is travel time from intersection i to intersection i+1 required by the vehicle with the highest speed on an outbound (inbound) path; t_s ($\bar{t}_s$) is the travel time from intersection i to intersection i+1 required by the vehicle with the lowest speed on an outbound (inbound) path; $F = 1/(1+\kappa T_i)$ and κ is an adjusting factor and is set to 0.35 as in Robertson (1969). Thence, the second proposed model, named RM2, is given by replacing the constraints (26)–(27) in RM1 with (28)–(29).

The following result formalizes the connection between model RM1 and model RM2.

Theorem 4.1: *When all traffic is assumed to travel at speed $v - d\kappa$, for which $0 < \kappa < v/d$, model RM2 is equivalent to model RM1.*

Proof: Since Equations (28) and (29) are used to substitute Equations (26) and (27), it is not hard to see that the dispersion constraints reduce down to the free-flow constraints through the following transformation:

$$t_f = \frac{d}{v - d\kappa}, \quad \text{and} \quad t_s = t_f$$

Theoretically, for the above to hold, we impose the condition

$$0 < \kappa < \frac{v}{d}$$

■

Hence, it is obvious that constraints (26)–(27) can be deemed a special case of constraints (28)–(29). Then we have the following result.

Corollary 4.2: *The feasible domain of RM2 is larger than that of RM1, viz.,*

$$\mathcal{F}(RM1) \subset \mathcal{F}(RM2) \tag{30}$$

and thus the objective function value for RM2 is bigger than that for RM1.

From the above, we can formalize the relationship among the proposed models and the base model in what follows

$$\text{RM2} \overset{t_f = \frac{d}{v-d\kappa} = t_s}{\rightarrow} \text{RM1} \overset{Z,\phi \text{constant}}{\rightarrow} \text{M2}$$

5. Real data

We conduct a real-world application on the proposed models. An arterial system, containing a highway ramp system and surface signalized intersections, in Chubei City, Taiwan, is chosen. Figure 2 shows the geographical topology for the test arterial system. Unlike most of the traffic systems, containing motorcycles and vehicles at the same time, in Taiwan, this particular system is chosen because it is a rarely seen pure-traffic system in that motorcycles are banned from entering. Moreover, this system has played a crucial role in accommodating the commuting traffic between Hsinchu city, Chubei city and the vicinities. Congestion during the rush hours has been long a serious problem and the current control strategy is no longer sufficient to control the over-saturated traffic. Thence, we value its importance and aim to provide a better control alternative that can help mitigate the congestions.

On-site investigations were carried out and traffic data were collected over a 4-hour rush-hour period (17:00–21:00) on 13 April 2013. Traffic volume data suggest five critical paths that contain most of the traffic over the planning horizon. Path 1 contains the traffic flow from the northbound off-ramp through the major arterial; paths 2 and 3 pass through the major arterial in opposite directions; and paths 4 and 5 are from minor legs of the surface signalized intersections to the major arterial. Paths 1

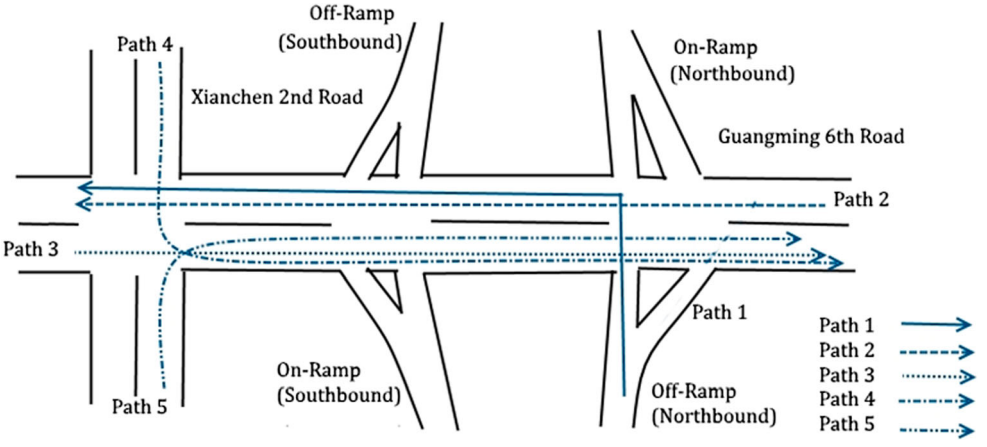

Figure 2. Geographical topology of the test network in Chubei, Taiwan.

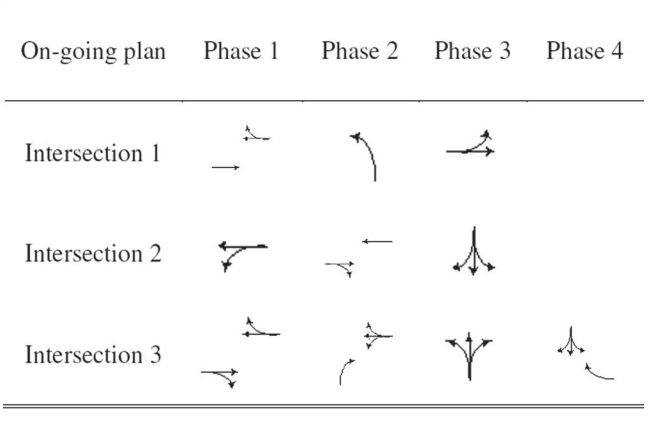

Figure 3. Design of phases of a cycle for the on-going timing plan.

and 2 are outbound paths, and paths 3, 4, and 5 are inbound paths. We label the three intersections, from right to left, as 1, 2 and 3, respectively.

For numerical implementations, we conduct both problem solving and traffic simulations for performance evaluations. For problem solving, we code up a C++ program connecting the Gurobi optimization solver for securing feasible timing plans for the proposed models introduced in Section 2. Obtained signal timing plans as well as the real traffic data then serve as the input to the traffic software integrated system (TSIS) for random simulations. We run 500 independent replications (due to the limitation of TSIS) and output the averaging performance measures. The official on-going timing plan (the one implemented by governmental transportation authority) as well as the one suggested in Yang, Cheng, and Chang (2015) are used for comparisons. Design of phases for the on-going plan is given in Figure 3.

6. Performance evaluations

For performance evaluations, we adopt the performance measures output from the TSIS software. Those measures include *delay control total*, *delay queue total* and *delay stop total*, all in unit of minutes. We compare both the path- and network-wise performance measures over a 4-hour time horizon, from 17:00 to 21:00, with the four timing plans. For alternative plans, the on-going timing plan serves as the initializing solution in the optimization procedure. After obtaining the results from the optimization solver, we input both timing plans and the traffic data into TSIS and repeat the simulation for 500 times. The reason that we cannot run more replications resides mainly in the limitation of TSIS. Simulation results are summarized and we exploit the law of large numbers (LLN), *viz.,*

$$\frac{\sum_{i=1}^{n} X_i}{n} \xrightarrow{P} \mathbb{E}[X]$$

to obtain the mean performance. In other words, we expect

$$\lim_{n\to\infty} \mathbb{P}\left\{\left|\frac{\sum_{i=1}^{n} X_i}{n} - \mathbb{E}[X]\right| > \epsilon\right\} = 0 \tag{31}$$

for some $\epsilon > 0$.

6.1. Path-wise performance

6.1.1. Delay control

Figure 4 shows the path-wise comparisons of the four timing plans on the control delay per vehicle over the time horizon. Obviously, the proposed models outperform both the official on-going and Yang's timing plans. Table 1 lists the relative improvements of the timing plans compared to the on-going plan on the path-wise aggregate control delay per vehicle (summing delays of all paths). We can see that, while the improvements in Yang's model are around 10%, the improvements from both RM1 and RM2 are around 26% $\sim$ 40%.

From both the figure and the table, we observe that even though, path-wisely, results from RM1 and RM2 do not reveal any superiority of anyone of the two plans (see Paths 2, 3 and 4), RM2 is a better model than RM1 from an aggregate perspective. This said, the incorporation of the dispersion constraints does bring improvements to the situation, compared to the free-flow setting in other models. As a matter of fact, this can be expected because, in reality, the free-flow speed can hardly be reached and the use of constant travel time is far unrealistically ideal.

From the results for Paths 3–5 in Figure 4, we see that, for the on-going and Yang's plans, the control delay per vehicle is trending upwards as time evolves. From the socioeconomic perspective, this may be because the inbound direction leads to the residential area as well as the Highspeed railway station in Chubei city. Scientifically, echoing Theorems 3.2 and 3.3, both the on-going and Yang's plans

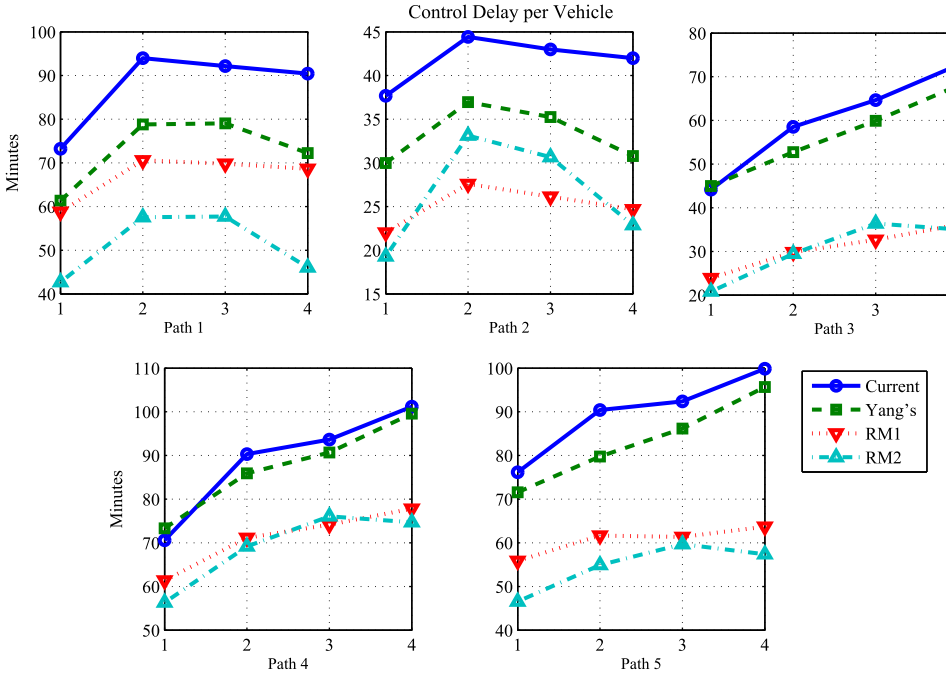

Figure 4. Path-wise comparison of the control delay per vehicle from 17:00 to 21:00.

Table 1. Relative improvements in alternatives plans compared to the on-going plan with respect to the three measurements.

Control delay	17:00–18:00	18:00–19:00	19:00–20:00	20:00–21:00
Yang's	6.8%	11.5%	8.9%	9.8%
RM1	26.4%	30.9%	31.5%	33.3%
RM2	38.4%	35.3%	32.5%	41.8%
Delay queue	17:00–18:00	18:00–19:00	19:00–20:00	20:00–21:00
Yang's	11.1%	16.8%	10.9%	10.6%
RM1	24.1%	27.7%	27.9%	31.1%
RM2	48.2%	35.3%	32.4%	50.1%
Delay stop	17:00–18:00	18:00–19:00	19:00–20:00	20:00–21:00
Yang's	11.1%	17%	10.9%	10.6%
RM1	24.6%	28.1%	28.3%	31.6%
RM2	48.8%	41.9%	35.5%	50.9%

have their common cycles and lengths of phases fixed. Lack of flexibilities in the timing operations leads to such consequences. Hence, these observations highlight the value of the proposed models in the sense that the proposed models possess the potential ability to mitigate such predicaments by introducing more flexibilities to the timing operations.

6.1.2. Delay queue and stop

Figure 5 shows the path-wise comparisons in terms of the delay queue total on the four timing plans. Overall, the improvements from the results for the proposed models RM1 and RM2 are significant, except for Path 2 and Path 4. We conjecture that this may be a consequence of leveraging the traffic volume among the paths. More specifically, if we look at the queue lengths in the rest paths (Paths 1, 3, and 5), the queue lengths are improved significantly. Yet, the signal timings for Path 2 and Path 4 are conflicting with these paths. Thence, the resulting growing trends in the queue lengths in Path 2 and Path 4 stems from more green time (and thus more red time for themselves) for the conflicting traffic. Since the models are path-based, the weighting parameters φ in the objective function may

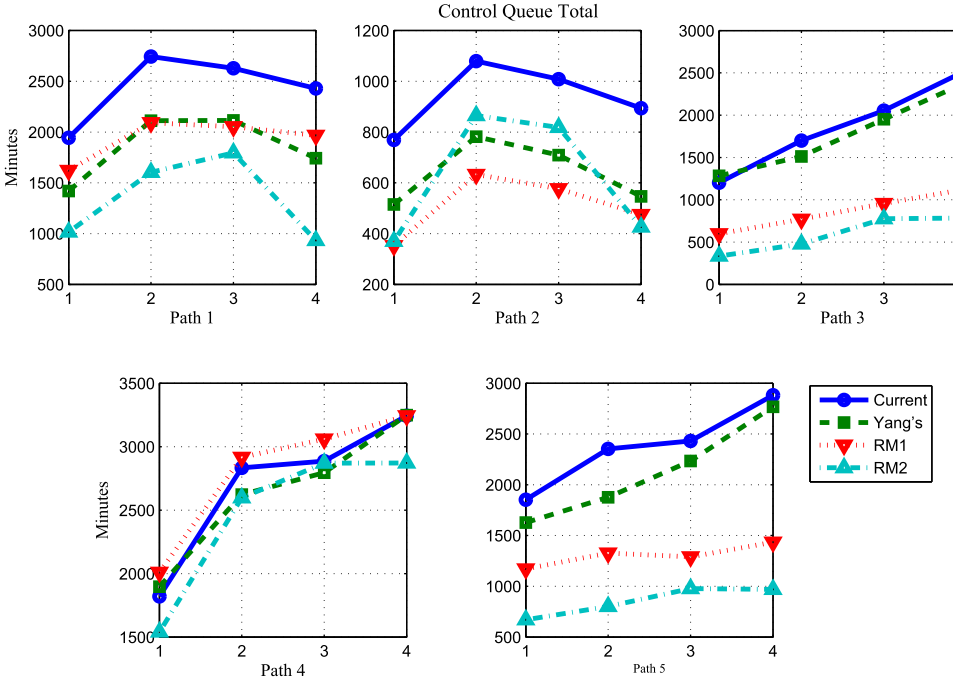

Figure 5. Path-wise comparison on the delay queue from 17:00 to 21:00.

also play some role in this situation. In other words, should some of the paths are of greater practical concern, more weights can be set with respect to those paths. In our case, since all φ are set equal, the solution suggests that Path 2 and Path 4 are leveraged, thereby making Paths 1, 3 and 5 relatively more important.

We look at the aggregate results as well. Table 1 lists the relative improvements from the alternative plans compared to the on-going one. Numerical evidences suggest RM2 outperforms the rest models. Improvements from Yang's model are around 10% $\sim$ 15% on the performance measures, while the improvements from the proposed models are around 3 $\sim$ 5 times better than Yang's. Again, such significant improvements should be expected, according to Theorems 3.2 and 3.3. If we look at the improvements during the period 19:00–20:00, in most cases, the improvement rates are comparatively smaller than others. This may be because working people are off duty and the traffic naturally gets intense, and thus more queues are expected, see also Figures 5 and 6.

From the perspective of delay stop output from TSIS, the improving trends are similar to those with the delay queue. Figure 6 shows the graphical evidences. Similar conclusions on Path 2 and Path 4 can be made. Aggregate results in this aspect also suggest that RM2 is the best alternative compared to others.

6.2. Network-wise performance

For network performance, we output the minute-by-minute simulation results for the above three measures, along with the number of trips per minute, in Figure 7. For the three measures, we can see that, as time evolves, model RM1 performs better than Yang's model, while RM2 remains dominating throughout the time horizon. The on-going timing plan, as expected, has the less satisfactory results.

As to the number of trips, RM2 still outperforms the rest models, with an average of 102.264 (standard deviation 15.2895) trips made per minute over the 4-hour time horizon. From Figure 7, a downward trend is observed for this particular measure. This, as a matter of fact, fits in with the results

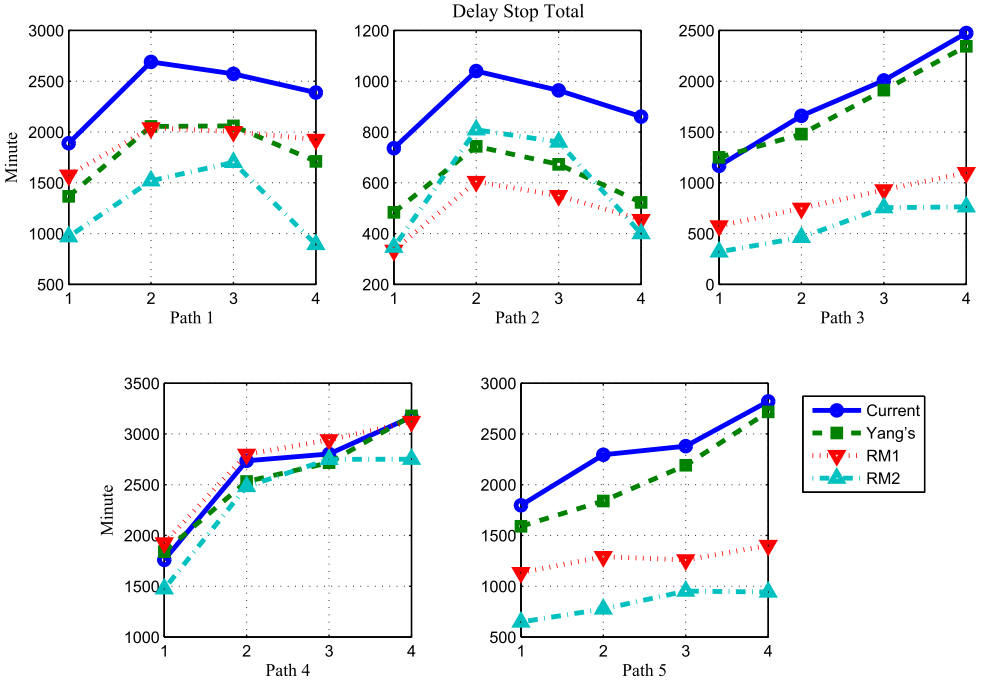

Figure 6. Path-wise comparison of the delay stop from 17:00–21:00.

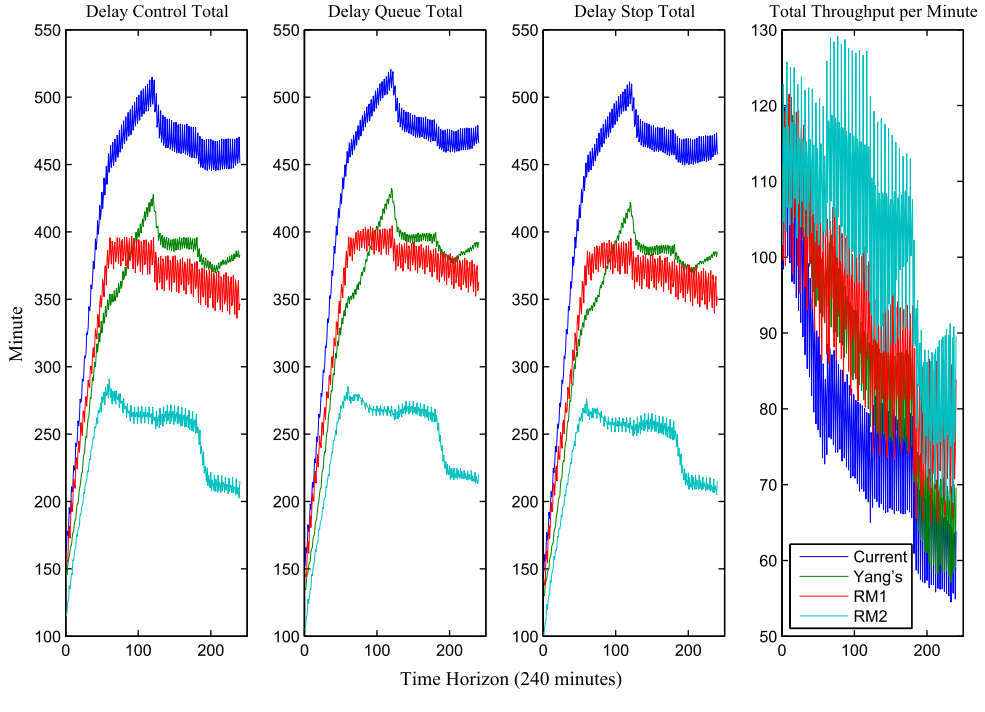

Figure 7. Simulation results of minute-by-minute performance measures over a 4-hour period.

Table 2. Gurobi results for four timing plans.

Plan	on-going Offset	Cycle = 180 Phase	Yang's Offset	Cycle = 180 Phase
Intersection 1	33	$\begin{pmatrix}1 & 2 & 3\\56 & 71 & 53\end{pmatrix}$	0	$\begin{pmatrix}3 & 1 & 2\\53 & 56 & 71\end{pmatrix}$
Intersection 2	3	$\begin{pmatrix}1 & 2 & 3\\56 & 69 & 55\end{pmatrix}$	0	$\begin{pmatrix}3 & 1 & 2\\55 & 56 & 69\end{pmatrix}$
Intersection 3	28	$\begin{pmatrix}1 & 2 & 3 & 4\\40 & 48 & 30 & 62\end{pmatrix}$	0	$\begin{pmatrix}4 & 3 & 2 & 1\\40 & 30 & 48 & 40\end{pmatrix}$
Plan	RM1 Offset	Cycle = 200 Phase	RM2 Offset	Cycle = 150 Phase
Intersection 1	73	$\begin{pmatrix}2 & 1 & 3\\61 & 87 & 52\end{pmatrix}$	62	$\begin{pmatrix}1 & 3 & 2\\55 & 39 & 56\end{pmatrix}$
Intersection 2	0	$\begin{pmatrix}3 & 1 & 2\\52 & 70 & 78\end{pmatrix}$	0	$\begin{pmatrix}1 & 2 & 3\\52 & 58 & 39\end{pmatrix}$
Intersection 3	50	$\begin{pmatrix}4 & 1 & 2 & 3\\57 & 57 & 46 & 40\end{pmatrix}$	47	$\begin{pmatrix}1 & 2 & 3 & 4\\34 & 43 & 30 & 43\end{pmatrix}$

Note that the first rows in the matrices correspond to the sequence of phases and the second to the lengths thereof.

for the delay queue and delay stop in the path-wise performance section. As time evolves, the volume of traffic grows, and therefore, as expected, the number of trips made per unit time is negatively correlated therewith.

Table 2 summarizes the results obtained from Gurobi optimization solver. We can see that, in the on-going and Yang's plans, the cycle lengths are fixed at 180 seconds. The optimization procedure, instead, suggests 200 and 150 seconds for model RM1 and RM2, respectively. Such results, once again, highlights the value of the proposed models that imposing flexibilities in the timing operations can help improve the system performance. Although theoretically the models become of more difficulty (the need to solve MIQCP), the hard work can be balanced off with the help and availability of exquisite optimization solvers nowadays.

From the cycle lengths, model RM2 requires the least time to complete a cycle, whereas model RM1 requires the longest. Since RM1 differs from Yan's in the aspects of cycle length and phase lengths, we think such a result may stem from the fact that more time is needed to accommodate the flexibilities resulting from relaxing the timing operations, while keeping the link travel time constant. On the other hand, model RM2 further relaxes the constant link travel time, a shorter cycle is then expected.

7. Concluding remarks and future directions

In this paper, we present two extensions of the path-based signal synchronization model proposed in Yang, Cheng, and Chang (2015). The first model RM1 relaxes the assumption that the ratios of phases, as well as the length of the common cycle, are fixed. Such a relaxation expands the solution space and therefore improvements can be expected, as proved in Theorem 3.3. The second model RM2 further relaxes the link free-flow speed assumption and incorporates the traffic flow dispersion module for better estimating the link travel times. Numerical evidences suggest significant improvements with the proposed models. Further, network-wise performance measures suggest that RM2 is the best alternative among all models, whereas there is no overall superiority between RM1 and RM2 in the path-wise sense.

Here we remark on the (possibly unfair) comparisons with the timing plan suggested by Yang, Cheng, and Chang (2015). There might be readers who may question if the comparisons are made on an equal basis. The answer is positive and, to be rigorous, we provide two theorems (Theorems 3.2 and 3.3) to show that theoretically our claim is true. Hence, even though there are differences in

the computing environments and/or simulation software, the results we present in this paper are convincing both numerically and theoretically.

Last but no least, discussions of the signal synchronization problem still are limited by assuming that the design of the phases comprising a cycle is pre-defined. A potential future research direction resides in the optimal design of phases for signalized intersections. A proper design of phases can certainly help improve the LoS of both the underlying signalized intersections and the entire network associated.

Acknowledgments

We sincerely thank the referees for their insightful comments that complete the paper in its current form. We also thank Dr. Ming-De Tseng, Dr. Zhibin Deng (UCAS, China) and Dr. Ziteng Wang (NIU, USA) for their professional opinions so helpful for our work.

Disclosure statement

No potential conflict of interest was reported by the authors.

Funding

This article was supported by Ministry of Science and Technology (MOST), Taiwan [grand numbers MOST-105-2622-8-009-008 and MOST-104-2221-E-009-162].

References

Chang, E. C., S. L. Cohen, C. Liu, N. A. Chaudhary, and C. Messer. 1988. *Maxband-86: Program for Optimizing Left-turn Phase Sequence in Multiarterial Closed Networks*. Transportation Research Record. 1181.

Dai, G., H. Wang, and W. Wang. 2015. "A Bandwidth Approach to Arterial Signal Optimisation with Bus Priority." *Transportmetrica A: Transport Science* 11 (7): 579–602.

Gartner, N. H., S. F. Assman, F. Lasaga, and D. L. Hou. 1991. "A Multi-band Approach to Arterial Traffic Signal Optimization." *Transportation Research Part B: Methodological* 25 (1): 55–74.

Gartner, N. H., and C. Stamatiadis. 2002. "Arterial-based Control of Traffic Flow in Urban Grid Networks." *Mathematical and Computer Modelling* 35 (5–6): 657–671.

Jeroslow, R. G. 1973. "There Cannot be Any Algorithm for Integer Programming with Quadratic Constraints." *Operations Research* 21 (1): 221–224.

Little, J. D. C. 1966. "The Synchronization of Traffic Signals by Mixed-integer Linear Programming." *Operations Research* 14 (4): 568–594.

Morgan, J. T., and J. D. C. Little. 1964. "Synchronizing Traffic Signals for Maximal Bandwidth." *Operations Research* 12 (6): 896–912.

Pardalos, P. M. 1991. "Global Optimization Algorithms for Linearly Constrained Indefinite Quadratic Problems." *Computers and Mathematics with Applications* 21 (6–7): 87–97.

Robertson, D. I. 1969. TRANSYT: A Traffic Network Study Tool.

Roess, R. P., E. S. Prassas, and W. R. McShane. 2011. *Traffic Engineering*. 2nd ed. Upper Saddle River, NJ: Pearson.

Shoufeng, L., L. Ximin, and D. Shiqiang. 2008. *International Colloquium on Computing, Communication, Control, and Management*. Guangzhou: ISECS.

Stamatiadis, C., and N. Gartner. 1996. "Multiband-96: A Program for Variable-bandwidth Progression Optimization of Multiarterial Traffic Networks." *Transportation Research Record: Journal of the Transportation Research Board* 1554: 9–17.

Tseng, M.-T. 2012. "Radar Vehicle Detection and Shockwave Techniques for Signal Control of Closely Spaced Intersections", Doctoral diss., Department of Transportation and Logistics Management, College of Management, National Chiao Tung University, Taiwan.

Yang, X., Y. Cheng, and G.-L. Chang. 2015. "A Multi-path Progression Model for Synchronization of Arterial Traffic Signals." *Transportation Research Part C: Emerging Technologies* 53: 93–111.

Zhang, C., Y. Xie, N. H. Gartner, C. Stamatiadis, and T. Arsava. 2015. "AM-Band: An Asymmetricalmulti-Band Model for Arterial Traffic Signal Coordination." *Transportation Research Part C: Emerging Technologies* 58: 515–531.